I give permission for public access to my thesis and for any copying to be done at the discretion of the archives librarian and/or the College librarian.

_____ _____

Signature Date

ABSTRACT

The global carbon cycle involves the annual movement of gigatons of carbon between reservoirs. Carbon moves into the atmospheric reservoir from sources such as fossil fuel burning and plant respiration, and moves out of the atmosphere into sinks such as deep ocean waters and burial in sediments. Rivers play an important and poorly understood role in the movement and storage of carbon.

The Rio Beni of Bolivia travels through an extreme altitude range, from its source in the Andes Mountains down to the Amazonian lowlands. The movement of organic carbon (OC) through its watershed is of particular interest due to the river's sequestration of massive amounts of OC in its foreland basin through sediment burial associated with La Niña climate cycles.

In this study, lipids, specifically long-chain *n*-alkanoic acids (fatty acids, FAs) from plant waxes, were used as biomarkers (tracers) for plant-derived OC. The characteristic stable isotope patterns of these plant-derived compounds can be compared to the patterns found in sediments. Stable isotopes exhibit characteristic

patterns of depletion and enrichment based on elevation. The ratio of carbon-13 to carbon-12 is enriched with increasing elevation, while the ratio of deuterium to light hydrogen ($^{2}H/^{1}H$) is depleted. This relationship between stable isotope fractionation and altitude makes it possible to use isotopic analysis to trace the FAs (and by extension, OC) found within sediments to their elevation of plant origin within the watershed.

The expected trends of enrichment and depletion are evident in plants in the Rio Beni, on the order of 0.5-0.6‰/1000m for carbon, and -8.2‰/1000m for hydrogen, though the variability in isotopic values between individual plants is large for both isotopes. This interplant variability is caused by a variety of factors including differences in biosynthetic pathway (i.e. C3 vs. C4) and climate.

The isotopic signatures of the plant samples were compared to those for sediment samples. The sediment samples were separated into two size fractions which should have distinct chemical properties. The <63 μm fraction is generally more enriched in FA $\delta^{13}C$ than the >63 μm fraction; this suggests the OC in the small fraction originated higher in the watershed or in plants which follow a C4 biosynthetic pathway, while the >63 μm fraction is from a more local, C3-derived source. The initial sediment δD data appear to support this finding, with the large fraction of one sediment sample exhibiting δD enrichment relative to the <63 μm fraction consistent with lowland C3 plant origin. Further δD values for more sediment samples will be required to confirm these preliminary results.

AN ISOTOPIC STUDY OF AN ANDEAN WATERSHED: CARBON CYCLING IN THE RIO BENI

by

Sarah E. Knudsen

A Paper Presented to the

Faculty of Mount Holyoke College in

Partial Fulfillment of the Requirements for

the Degree of Bachelor of Arts with Honor

Department of Chemistry

South Hadley, MA 01075

May 10, 2011

This paper was prepared

under the direction of

Professor Angela F. Dickens

for eight credits.

ACKNOWLEDGEMENTS

Thank you to Professor Angela Dickens for inviting me into her lab, introducing me to the fascinating world of organic biogeochemistry, and guiding me through the process of learning to conduct scientific research.

I greatly appreciate the generosity of Professors Jill Bubier and Desiree Plata for taking time out of their busy schedules to be on my thesis committee and provide me with valuable feedback on this project.

Thank you to the Mount Holyoke College Chemistry Department – faculty, staff, and students – for being my home over the past three years. More specifically, thanks to my labmates, Bokyung Kim and Hailey Riggan. There's nothing like the combination of good friends waiting for solvents to dry, large expanses of glass and permanent markers to make research fun!

I'd like to thank all of my friends and family for putting up with me and listening to me complain through the process of research and writing that led to this thesis. Though it may not have been obvious at times, I have loved (almost) every minute of the process, and I could not have done it without your support.

A special thank you to my sister-by-choice Laura Ridenour for devoting her lunch breaks to reading drafts and being my grammar fairy. Any remaining errors are my own fault. The presence of parentheses in this final draft is against her will (and best efforts).

Most importantly, I would like to thank my father, Stephen Knudsen, for his support on my long path to Mount Holyoke and for his reassurance that I was not insane for choosing to write a thesis.

TABLE OF CONTENTS

TABLE OF FIGURES

TABLE OF TABLES

CHAPTER 1: INTRODUCTION

I. The carbon cycle

Carbon is one of the basic building blocks of life and is found in all organisms. The movement of carbon between different environments and between different chemical forms is cyclical, with the same carbon being repeatedly transformed and moved on a variety of time scales.[1] These transformations and movements are inextricably interconnected, and together they make up what is commonly referred to as the *carbon cycle*. Atmospheric levels of carbon-based greenhouse gases such as methane (CH_4) and carbon dioxide (CO_2) are intimately linked to the carbon cycle, so a better understanding of the processes and mechanisms involved in the carbon cycle may help us to understand and address climate change.[1, 2] This is a major motivating factor behind studies of the mechanisms and processes of the carbon cycle.

The carbon cycle can be considered as an interconnected system consisting of the movement of carbon between reservoirs (Figure 1). While the amount of carbon in a specific part of the system at any one time may vary

somewhat, the total amount of carbon in the system is almost constant and can be thought of as the carbon budget. The largest carbon reservoir is found in the ocean, with the atmosphere and soils serving as other large reservoirs.[1]

Reservoirs of carbon can be classified as sources or sinks relative to the atmosphere. In a sink, net carbon input to that reservoir exceeds carbon output, while sources have higher output than input.[3] Sources of carbon to the atmosphere include the burning of fossil fuels as well as other processes that release carbon-based gases to the air, such as land use change.[1, 3] Sinks of carbon are reservoirs that provide long-term carbon storage or sequestration.[3] The largest sink for atmospheric carbon is the world's oceans, while the largest land sinks are soils and vegetation.[1, 3, 4]

The movement of carbon between reservoirs is called a *flux*, and the rate and direction of fluxes may change due to a variety of factors, including changing the reservoir in which the carbon is resident, as well as the type of compounds (i.e. organic or inorganic) the carbon constitutes.[3, 4] The factors affecting the magnitude and rates of fluxes include human activity and climate change.[1] See Figure 1 for the scales of various sources and sinks, as well as the fluxes between them.

Carbon is found in both organic and inorganic forms. Atmospheric carbon is mostly found as CO_2 (inorganic), while in the ocean it primarily appears as bicarbonate (inorganic); in plants carbon is found in organic form, while in soils and rivers it is found in a mix of inorganic and organic forms.[1, 5] Inorganic carbon

(IC) is converted to organic carbon (OC) via processing by living organisms. IC in the atmosphere and soil can be fixed by plants and microbes through photosynthetic pathways to become OC, while respiration and other biological processes produce inorganic carbon from OC.[1]

Fossil fuels such as oil and coal formed thousands or millions of years ago from buried decayed organic matter, such as leaves.[1] Combustion of fossil fuels converts previously-sequestered OC to inorganic greenhouse gases such as CO_2, and leads to the release of the carbon to the atmosphere. Fossil fuel carbon was formerly a large and isolated sink, but burning causes this carbon to become part of the active carbon cycle. This increase in atmospheric greenhouse gases such as methane and CO_2 is a major driving force behind climate change.[2]

The largest sources of carbon to the atmosphere can be classified as anthropogenic, or originating from human activity, and non-anthropogenic, or originating from non-human sources. The most important anthropogenic contributions are the production and burning of fossil fuels. Waste management, cement production, biomass burning, land use change and agriculture (especially rice production) are among other important contributors to anthropogenic carbon release.[1, 4, 6] Non-anthropogenic sources include wildfires and the release of organic gases such as carbon dioxide and methane from melting glaciers and thawing permafrost.[4] It is important to note that while these sources are not directly anthropogenic, the rates at which they occur are being altered, generally increased, by climate change due to human activity.[2] In any case, the pooled

contributions of anthropogenic sources of carbon to the atmosphere account for approximately double the total non-anthropogenic input of organic carbon.[4]

Climate plays an important role in the function of carbon sinks and the wider carbon cycle. Feed processes inextricably link climate and carbon cycle fluxes: greenhouse gases in the atmosphere affect climate, and in turn, climate affects the amount of these gases released into the atmosphere.[7] For example, CO_2 and methane are released when thawing permafrost OC decomposes. The El Niño/La Niña climate cycle also affects global concentrations of atmospheric CO_2, with increased CO_2 release from the ocean (and potentially other aquatic sinks such as rivers) due to El Niño warming.[2, 4] The greenhouse gases released by warming may contribute to increased warming, in a positive feedback cycle.[7]

II. The role of rivers

Rivers play an important role in the carbon cycle, moving both inorganic and organic carbon between reservoirs. Further, sediment pools found in rivers act as major carbon sinks, sequestering huge amounts of carbon, particularly in their deltas and foreland basins (long, narrow valleys found parallel to mountain ranges).[6, 8]

Rivers do not serve as mere conduits of carbon to the oceans, but as dynamic processors of organic matter. The organic carbon found in rivers may come directly from land sources or derive from in-river production. Human activity such as mining and agriculture and natural processes such as landslides, floods and erosion lead to the movement of land-derived OC to rivers.[6] This non-

riverine OC may have been stored in soils or other sediments before entering the river system and been degraded or sorbed to minerals prior to its deposition in the river.[9] OC in rivers is found in both dissolved (DOC) and particulate (POC) forms. Also, DOC may sorb to suspended materials to become POC and vice versa.[9]

The water in rivers and floodplains in the lower Amazon basin are supersaturated in CO_2 relative to the atmosphere, and thus they act as a large source of CO_2 to the atmosphere when the CO_2 is outgassed downstream. It has been suggested that the outgassed carbon originates from organic matter transported from the upland portions of the watershed.[10] This organic matter decomposes as it travels downstream, producing some of the CO_2 that is then outgassed by the river. Other factors, such as root respiration in forests along the banks of rivers and the respiration of wetland plants, also contribute to the rise in partial pressure of CO_2 in rivers and the subsequent CO_2 outgassing.[10] Overall, it appears that much of the organic matter that enters rivers is not delivered unchanged to the oceans, but is instead processed in some way: degraded, sorbed to minerals, outgassed back to the atmosphere, or stored in sediments.[10-13]

There is a slower-than-expected rate of increase in atmospheric carbon.[14] However, current models of the global carbon budget disagree somewhat on the size of this discrepancy, which may be on the order of approximately 2.9 Pg carbon/year between the amount of carbon that can be accounted for by known sinks and the amount missing from the atmosphere. Rivers and their sediments are

one candidate for the residual terrestrial sink (also called the "missing sink") due to the massive amounts of OC that are sequestered with the burial of sediments.[12, 13]

At this time, little is known about the fate of sedimentary OC in rivers. For example, the quantity of it that is transported, and how far that quantity may travel. Additional questions include which sediment size fractions contain more and less degraded OC and the origin and scale of the large sedimentary OC deposits in foreland basins.

III. Biomarkers

Environmental samples contain complex mixtures of organic carbon from many sources, so measurements of bulk properties do not always provide clear answers about the origin or other properties of the organic matter within the sample. One approach to this problem is the use of biomarkers, which allow examination of properties of a specific type of OC that bulk analyses cannot target.

OC is composed of organic molecules, which are byproducts of the life processes of plants and animals. Some of these organic molecules persist beyond the death of the organism, unchanged or modified but still recognizable. Such identifiable compounds or molecular residues left behind by organisms are known as biomarkers if they can be reliably quantified and connected to their original source.[15]

Features of a biomarker such as its concentration, structure, and isotopic

signature can be compared to known and standard values to allow their use as tracers, or molecular proxies.[15, 16] If a such a biomarker is isolated from an environmental sample (for example, lignin, a biomarker produced by plants and isolated from a sediment sample) it is clear evidence of the presence of at least some of the material of interest in that environmental pool (e.g. plant-based carbon *is* present in the sediment). In simpler terms, the "fingerprint" of a biomarker compound found in an area of interest can be compared to the "fingerprint" of the same type of compound from a potential source.

A good biomarker is easily quantifiable, often through chromatography (gas or liquid) and mass spectrometry.[16] An ideal biomarker will be chemically inert and relatively resistant to degradation (or at least follow a predictable pattern of degradation), and it will have a known and traceable mechanism of production.

Biomarkers have applications in petroleum exploration, studies of climate change, archaeology and pollution monitoring among other fields.[15-20] Biomarker studies are conducted on land, in the atmosphere, and in the ocean. One of the many uses of biomarkers in ocean sediments involves tracking of compounds that originated on land to give insight into patterns of atmospheric circulation.[15] Analysis of biomarker compounds within the ocean can give insight into paleoclimatology and historical ocean conditions such as sea surface temperature (SST).[15] One example of the use of biomarkers on land is tracing the isotopic signature of compounds such as *n*-alkanes to allow estimation of past changes in vegetation due to the differing isotopic signatures of C3 and C4 plants.[17, 21] By

extension of the stable isotope techniques used for C3/C4 differentiation, biomarkers can be used as proxies to allow tracing sources of plant-derived organic matter, and from that information, tracing of the sources and movement of OC.

As proxies, biomarkers have certain limitations. In some cases, the same compound can stem from multiple sources. For instance, short-chain biolipids are commonly synthesized by microbial sources as well as the plant sources that investigators may wish to examine.[22] Further, the quantification of a biomarker is only as accurate as the standard to which it is compared; an inaccurate standard will lead to useless data and incorrect conclusions. Biomarkers may degrade with age, but the measurement of the degree of degradation can sometimes provide useful information rather than just posing a problem, allowing for estimation of the age of the compounds in question. However, this estimation may not be accurate, and resolution of the time scale of processes traced with biomarker proxies remains problematic.[15]

IV. Lipids as biomarkers

Lipids are widely distributed and have a variety of sources, as they are synthesized by plants, animals, and microorganisms. Lipids can be easily collected and quantified and exhibit characteristic concentration patterns. These factors combine to make lipids ideal biomarkers.[16, 22, 23]

Long-chain leaf wax lipids, *n*-fatty acids of general formula

$CH_3(CH_2)_nCO_2H$, are commonly used as biomarkers, proxies to trace the movement of plant-originated OC.[16, 22] Only the long-chain ($\geq C_{24}$) fatty acids are specific to plants; short-chain fatty acids are synthesized by microorganisms and other sources, such as plankton.[24] Long-chain lipids, such as those found in plant leaf waxes, are typically quite stable.[22, 25] These compounds are referred to by the number of carbons and the number of branches in the chain, for example, C26:0 (a 26-carbon chain with 0 branches). These fatty acids are generally derivatized to fatty acid methyl esters (FAMEs, Figure 2) before quantification.

Plant wax *n*-fatty acids exhibit a marked preference for the even-numbered carbon chains due to the biosynthetic pathway involved in their synthesis.[16, 25] The characteristic distribution of FAMEs for a particular plant can be described by the average chain length (ACL) and the carbon-number preference index (CPI). CPI is a measure of even-over-odd preference; a CPI in a reservoir similar to that found in plant samples suggests that the FAMEs were well-preserved in their travel from plant to reservoir.[26] Plants typically have high CPI and degraded materials and petroleum have low CPI.[26]

V. Stable isotopes

Stable isotopes are powerful tools for tracing processes within the carbon cycle, allowing us to track the movement of carbon from source to sink by comparison of the isotopic signatures of materials in the source and sink. This is because a variety of processes affect the isotopic ratios of different elements, so

by studying the ratios present in a particular reservoir, we can often infer the sources of that material or the processes it has undergone up to that point.[27] Stable isotope analysis of biomarkers can provide detailed information about the plant type and spatial origins of the organic matter that makes up an OC pool.

Isotopes are forms of the same element with different number of neutrons and, therefore, different atomic masses. Isotopes may be radioactive or stable; a stable isotope does not decay over time. Stable isotope measurements compare the amount of a heavier isotope to the amount of the lighter, generally more common isotope present in a sample.[27] The isotopic signature of a sample is reported as a delta (δ) value, which is calculated from the comparison of the measured isotopic ratio of the sample to a standard using the formula:

$$\delta = \left(\frac{R_{sample} - R_{standard}}{R_{standard}}\right) \times 1000$$

where R_{sample} is the molar ratio of the heavy to light isotopes in the sample studied (for the purposes of this study, R = $^{13}C/^{12}C$ or R = D/H), and $R_{standard}$ is the ratio measured in a physical standard. The units of δ are "per mil," parts per thousand. The standard for carbon is based on the Vienna Pee Dee Belemnite (VPDB), a Cretaceous marine fossil (*Belemnitella americana*), and the standard value for hydrogen is based on Vienna Standard Mean Ocean Water (VSMOW), a reference sample of ocean water.[27, 28]

The relative magnitude of fractionation effects is generally much larger for δD than for $\delta^{13}C$ because the mass difference between D and H is so great (D is

twice as heavy as H), while the difference between ^{13}C and ^{12}C is much smaller. This is because isotope fractionation generally increases as the relative mass differences between the isotopes of an element increase.[27] Therefore, δD signatures may vary by as much as 100's of ‰, while $\delta^{13}C$ may vary by only 20-30‰. This means that the same 20‰ variation if seen in $\delta^{13}C$ is relatively more important than it would be in δD.

Variations in stable isotope ratios come about through a variety of processes. The bonding in compounds containing heavy isotopes is stronger, making that molecule more difficult to break, leading to slower reaction rates. This leads to *kinetic* fractionation. *Equilibrium* fractionation arises when the physical properties of molecules made up of the heavier isotope vary from those of the lighter isotope. For instance, heavier molecules may diffuse more slowly through leaf surfaces.[27, 28] The isotopic signature of the atmospheric CO_2 in the plant's growth area will affect its $\delta^{13}C$ signature, and climatic factors such as high or low rainfall may affect its δD signature.[29, 30]

Altitude also has an effect on the distribution of stable isotopes in plant tissue.[29, 31] The $\delta^{13}C$ value of plants is enriched with increasing elevation due to a combination of factors including the lower temperatures and aridity typically found at higher elevations, as well as the effects of lower atmospheric pressure on plant metabolism.[29] On the other hand, δD values are significantly *depleted* with increasing elevation. Plant tissue δD values depend largely on the δD value of their growth water,[31] but δD and $\delta^{13}C$ values of compounds found in plant tissues

also vary depending on the biosynthetic pathway employed by the plant.[21, 29, 32, 33]

There are observable differences in the $\delta^{13}C$ and δD signatures of plants depending on whether they follow a C3 or C4 biosynthetic pathway – C4 grasses typically exhibit $\delta^{13}C$ and δD enrichment relative to C3 plants.[12, 21, 33, 34] The magnitude of these differences depend on the isotope; the magnitude of the $\delta^{13}C$ effect is typically smaller than that observed for δD, but relative to other fractionation effects the effect of biosynthetic pathway is less important for δD than for $\delta^{13}C$.[35] The δD values of C4 plants may be about 20‰ more enriched in D than those of C3 plants,[34] while the $\delta^{13}C$ signature of C4 plants is enriched by approximately 15‰ relative to C3 plants.[21] Climate also plays a role in the δD and $\delta^{13}C$ signatures of plant lipids, with a warmer, drier environment leading to greater enrichment in D and depletion in ^{13}C.[29, 34, 36]

VI. The study

This study addresses questions related to the movement of OC within the watershed, specifically, where in the watershed does OC deposited in the foreland basin originate? How is OC processed on its journey from source to sink? To address these questions, plant samples from the upper portion of the watershed were analyzed for their lipid concentration distributions as well as their compound-specific lipid $\delta^{13}C$ and δD signatures. These data should allow examination of the effect of altitude-based isotope fractionation during plant biosynthesis in the Rio Beni watershed. The same analyses were then carried out

for a sediment core from the Rio Beni floodplain. The plant and sediment isotope results were compared in an attempt to use the elevation effects on plant lipid signatures to determine which part of the watershed serves as the origin of the lipid biomarkers found in floodplain sediments. Analysis of the results should lead to a better understanding of the dynamics of carbon transport in the watershed and of the links between source and sink.

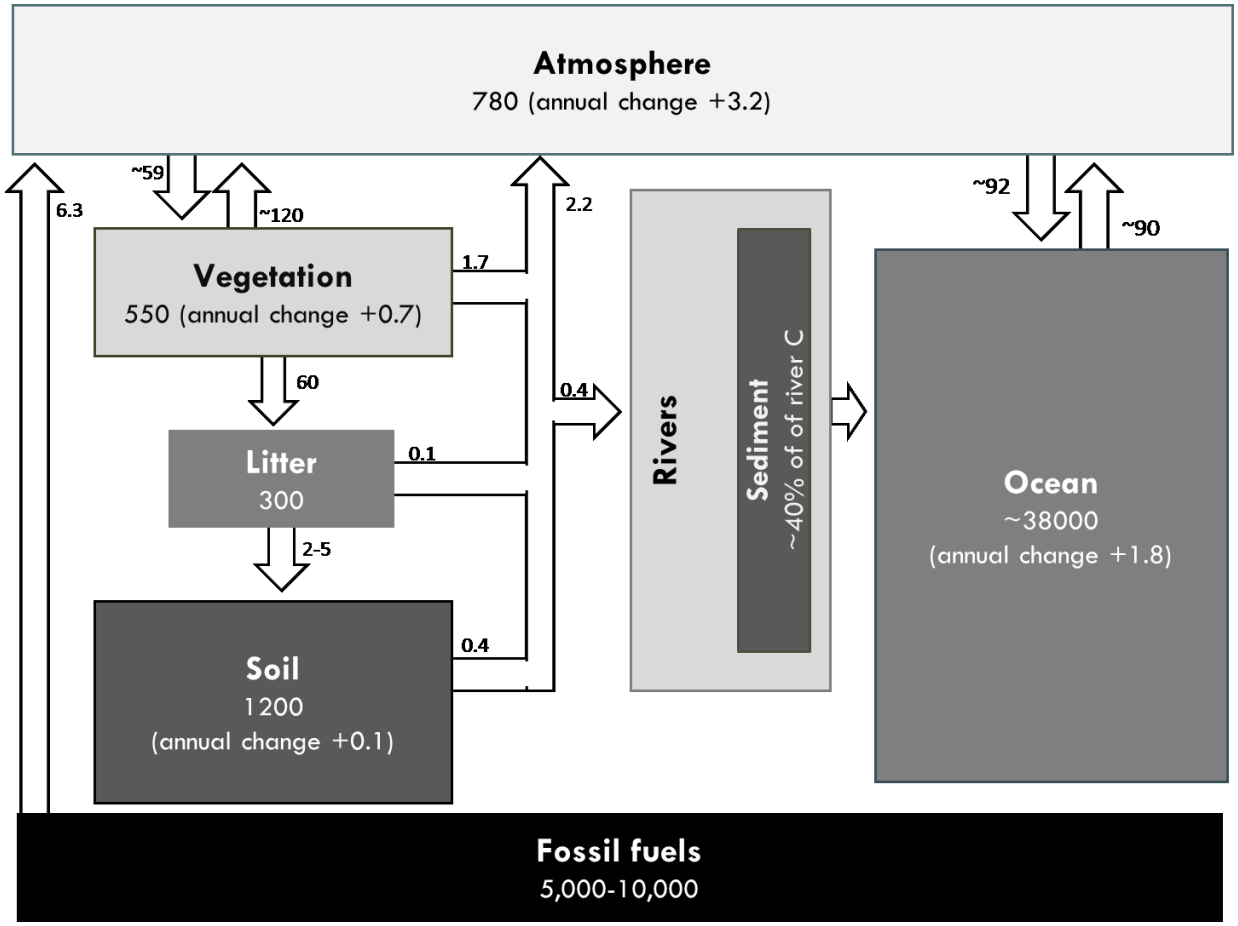

Figure 1: The global carbon cycle. The boxes represent reservoirs of carbon, while the arrows represent fluxes, or the movement of carbon between reservoirs. The exact breakdown of contributions to the flux from land sources to rivers is unknown. Units in petagrams (Pg, 1Pg = 10^{15}g) for reservoirs and Pg/year for fluxes. Data compiled from various sources.[3, 6, 12]

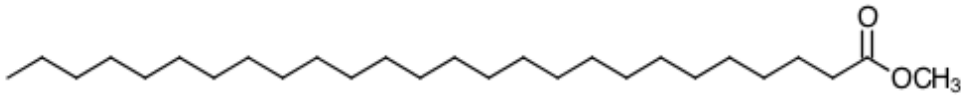

Figure 2: A C26:0 FAME (fatty acid methyl ester)

CHAPTER 2: STUDY SITE

I. Physical features

The Rio Beni, a major tributary of the Rio Madeira, itself a tributary of the Amazon River, flows from its source in the high Andes (elevation ~6400m) of Bolivia down to the Amazonian floodplain (~200m) (Figure 3).[37] The Beni drains a 70,000 km^2 area of the Bolivian Andes across approximately 50,000 km^2 of floodplain, and deposits on the order of 100 Mt/yr of sediment in the foreland basin floodplains.[38] The presence of a foreland basin in the Rio Beni watershed is an important part of the motivation for this study; foreland basins can store huge amounts of sediment, so it should be a major sink of carbon, sequestering large amounts of OC associated with sediments.[8]

There are frequent floods in the region; 11 major floods were recorded in the period from 1967-2003.[37] High water levels connected to major sediment discharge into the river occur on an annual basis during the warm months (December through April), with peak flow during January through March.[37] Multi-year ENSO (El Niño/Southern Oscillation) cycles also affect downstream

sediment delivery; the cold phase of this climate cycle (La Niña) causes higher than normal rainfall at the higher elevations in the watershed, causing the Rio Beni to flood. This flooding carries massive volumes of sediment down the river, and then deposits that material in the foreland basin floodplains.[38]

II. Vegetation

The watershed hosts a variety of plant types, with significant variation in the species present at different elevations. At high altitudes, the largely C3 altiplano (highland plains) and puna (grassland steppes) predominate. At lower elevations, the ground cover is mostly forest with pockets of grassland.[39, 40] C4 grasses are generally found only at elevations below ~2000m in this watershed.[40]

III. Transport of organic matter

Previous studies have characterized the bulk carbon transported by the river from the uplands to the floodplain. Hedges *et al.* found that the mean size of particulate organic matter (POM) in the river decreased with distance downstream from the river's source, potentially indicating processing of material from the uplands is occurring in the river.[41] The increase in degradation of OC with distance downstream from the river's source seen by Hedges and a variety of coworkers[11, 12, 41] also suggests processing of OC within the river. This raises the questions of how much of the OC that enters the river survives and how much of the OC buried by the river's sediments is from the higher portions of the watershed.

Size fractionation of POM prior to analysis is useful because it separates particles that typically follow different pathways through the environment. Prior studies have found separation at 63 μm to be particularly useful in this watershed.[11, 19, 39] The sedimentary coarse particulate organic matter (CPOM; >63μm) and fine particulate organic matter (FPOM; <63μm) in the river exhibit different chemical and biochemical compositions; CPOM appears to be recently produced matter rich in C3 plant material, while FPOM is generally older and sorbed to sediments.[39, 41, 42]

OC $\delta^{13}C$ values within the river are enriched at higher elevations but change, becoming more depleted downstream.[39, 41] This leads to questioning of what factors might cause this isotope effect. The ^{13}C enriched matter may be lost, or still be present with its signal diluted by the addition of low-altitude ^{13}C-depleted OC. The amount of highland OC that survives transport and is buried in the flood plain versus the amount lost to outgassing and remaining within the river is another open question.

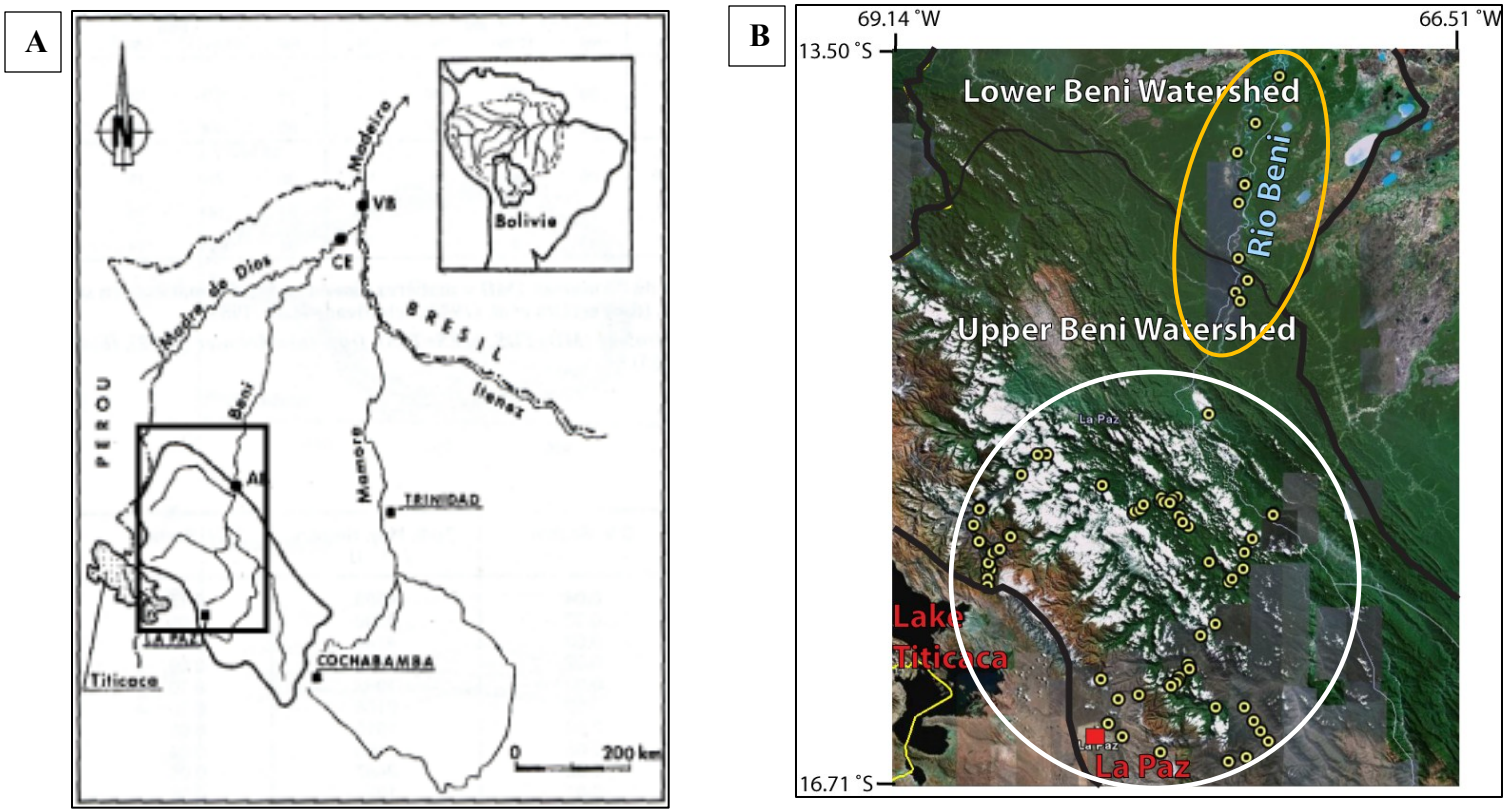

Figure 3: (a) The location of the Rio Beni watershed within South America; adapted from Guyot et al.[43] *(b) The study site. Small yellow circles represent sampling sites. The sites within the large white circle are locations of plant sampling within the upper watershed, while the sampling sites within the gold oval are sites of sediment core collection (this study analyzed a subset of the plant and sediment core samples marked here). Figure adapted from A. Aufdenkampe's figure from Google Earth.*

CHAPTER 3: MATERIALS AND METHODS

I. Sample collection and preparation

Plant samples were collected from the upper watershed and placed in plastic bags. They were air dried while on the field trip, then oven dried at 60 °C upon return to the lab. Several species were collected from each site and if possible included several tissues and individuals from each species. Each plant species sample was ground to a fine powder in a mill. A total of 30 plant samples (26 C3 plants and 4 C4 plants) were processed.

A sediment core was collected from the lower watershed (14.1558629° S, 67.5436488° W) with a 1.5 m push corer that collected the sample within a plastic sleeve. The core sleeve was sealed airtight immediately after collection and stored in a cold room until sectioning, which involved cutting the core at 2 cm intervals and drying the samples in an oven at 50 ºC. Another sediment ("bank deposit") was collected from an internal floodplain (13.50749° S, 67.27670° W) deposit about ten days after the sediments were deposited in a flood. Dried sediments were then homogenized, and the bank deposit sediment as well as each horizon

from the sediment core was wet sieved through a 63 μm stainless steel sieve. The two size fractions were freeze-dried and homogenized in their vial using a spatula.

II. Elemental and isotopic analysis

Bulk carbon elemental and stable isotopic analyses for the plant samples were carried out. Briefly, subsamples of each plant and sediment sample were wet with nanopure water and fumed with hydrochloric acid vapors for 18 hours, effectively removing carbonates while minimizing potential contamination of N due to ammonia absorption into the acid. Subsamples were analyzed in batches on an Elemental Analyzer (Costech ECS 4010) interfaced with an Isotope Ratio Mass Spectrometer (Thermo DeltaPlus XP). Standard curves for the elemental and isotopic analysis were created for each batch using 8 or 9 isotopically enriched (+37.63‰) and depleted (-26.39‰) L-glutamic acid standards over a range of carbon masses that encompassed the subsample masses. Stable carbon isotope ratios, reported using $\delta^{13}C$ notation, were normalized relative to the Vienna Pee Dee Belemnite standard using the approach and values provided in Coplen *et al.*[44]

Bulk isotopic analysis of the sediment samples was performed after acidification using the method outlined in Whiteside *et al.*[45] Briefly, samples underwent vapor phase acidification with concentrated HCl at 60-65 ºC for 60-72 hours and were dried at the same temperature for ~24 hrs. Samples were analyzed using a Carlo Erba 1108 elemental analyzer (EA) interfaced via a Finnigan-MAT Conflo-II open split device to a DeltaPlus isotope-ratio-monitoring MS; they were

compared to reference (NBS-19 and N1) and standard (a well-characterized glycine) samples.

III. Lipid analysis

The dried, finely-crushed plant samples and size-fractionated sediment samples were then subjected to microwave-assisted total lipid extraction (TLE). Briefly, a small mass of each sample was weighed into a Teflon extraction vessel, and 20 mL of a dichloromethane:methanol solution (9:1 by volume) was added to each. These vessels were then subjected to microwave-accelerated extraction using a CEM MARS system for 15 minutes at 100 ºC. After cooling, the TLE's were filtered through GF/F filters and then saponified using 6% KOH in methanol at 80 ºC for two hours.

After addition of environmental grade water and NaCl, the pH of the TLE's was brought to between 1.5 and 2 using HCl to ensure all organic acids were protonated and thus soluble in organic solvents. A liquid-liquid extraction was then performed using a 4:1 solution of hexane and dichloromethane. The extract was dewatered with combusted sodium sulfate and then transesterified under N_2 atmosphere at 70°C for 12-18 hours using a 95:5 mixture of isotopically-characterized methanol and 12N HCl. Transesterified samples were extracted with hexane after the addition of water. The extract was dried with sodium sulfate, and the total sample volume brought to exactly 1 mL before quantification by GC-FID as described below.

After initial quantification, the transesterified TLEs were purified using a glass Pasteur pipet as a column. The column was filled with approximately 4 cm of 5% deactivated silica gel (Fisher Scientific S734-1 100-200 mesh). Four 4 mL fractions were collected: a non-polar fraction (in hexane; primarily *n*-alkanes), a FAME fraction (in 2:1 hexane:dichloromethane), a polar fraction (dichloromethane with a little methanol), and a methanol fraction. The hexane, FAME, and polar fractions were then analyzed using GC-FID as described below.

FAMEs were quantified using an Agilent Technologies 6890N GC-FID by comparison to an external standard containing short-chain FAMEs (even carbon-number FAMEs in the range of nC$_{14}$-nC$_{24}$). An additional external standard was used for qualitative comparison to locate peaks longer than C$_{24}$. The GC was equipped with a Restek Rxi-1ms capillary column (30m x 250 μm x 0.25 μm). 1 μL of sample was injected onto the column via a splitless injection. The oven was ramped to 150 ºC at 30 ºC/min, then to 250 ºC at 8 ºC/min, and finally increased to 320 ºC at 4 ºC/min, which was held for 5 minutes. The H_2 carrier gas flow was held constant at 3 mL/min for the course of the entire run.

IV. Isotopic analysis of FAMEs

All FAME samples were analyzed for compound-specific ^{13}C and D ratios at Woods Hole Oceanographic Institution. Samples were analyzed in triplicate for δ^{13}C and in duplicate for δD. All data were corrected for the change in isotopic signature due to addition of a methyl group during transesterfication, so values

reported are for the fatty acids.

For ^{13}C analysis, the samples were injected using a Gerstel PTV (programmable temperature vaporizing) injector port operated in solvent venting mode, with an injection at 40 degrees with a 15 second hold, then programmed to increase at a rate of 12 ºC/second to 350 ºC and hold for 3 minutes. Solvent was vented at 30 mL/min for 15 seconds, after which all flow was directed to the column and the sample was transferred. The HP 6890 GC was equipped with a CP-Sil 5CB Low Bleed-MS (60m x 0.25 mm internal diameter x 0.25 μm phase) column, with a He carrier gas flow rate of 1 mL/minute. The temperature program was to hold at 60 ºC for 3 minutes, increase at a rate of 50 ºC/minute to 160 °C (no hold), then continue increasing at a rate of 3 ºC/min to 340 and hold for as long as needed to fully elute all compounds. The GC was interfaced to the Finnigan-MAT DeltaPlus IRMS by a GC-Combustion III interface, modified after Goodman[46] to an integral fused silica combustion design. The reference gas value was calibrated against a suite of 9 compounds analyzed on the system. Instrument accuracy and precision for this suite are generally 0.3‰ or better.[47]

For deuterium analysis, samples were measured using an Agilent gas chromatograph coupled to a Thermo Delta V isotope ratio mass spectrometer via a pyrolysis interface (GC/TC) operated at 1430 °C. A DB-5MS (60 m x 0.25mm, film thickness 0.25um) and PTV injector operated in solvent vent mode were used. Peaks of propane reference gas were co-injected between standard FAMEs to obtain a daily external calibration. The RMS error for all external calibration

runs was 3.9‰ (n = 8). For analysis, the calibrated propane was co-injected as the reference standard.

V. Calculation of ACL and CPI

Average chain length (ACL) was calculated based on the concentrations of the FAs in the range of nC$_{24}$-nC$_{32}$ according to the formula

$$ACL = \frac{24(C_{24}) + 25(C_{25}) + 26(C_{26}) + 27(C_{27}) + 28(C_{28}) + 29(C_{29}) + 30(C_{30}) + 31(C_{31}) + 32(C_{32})}{24 + 25 + 26 + 27 + 28 + 29 + 30 + 31 + 32}$$

where the values in parentheses are the concentrations of that FA.

Carbon preference index (CPI) was calculated based on the concentrations of the even carbon number ($C_{even)}$ and odd carbon number (C_{odd}) FAs using the formula

$$CPI = \frac{\sum C_{even}}{\sum C_{odd}}$$

CHAPTER 4: RESULTS AND DISCUSSION

I. Plants

Bulk properties

Plant weight percent OC varied from 24.66% to 49.05% with no clear relationship between %OC and plant type or elevation (Table 1). With data available for only four C4 plants, it was not possible to discern a trend with elevation for their bulk $\delta^{13}C$ signatures. However, as expected, [21] they displayed uniformly high ^{13}C enrichment relative to C3 plants (Figure 4). C4 plant biomass typically averages ^{13}C depletion of -14‰ and C3 biomass typically averages -26 to -27‰ relative to VPDB.[21, 48] The values for C3 and C4 bulk material are close to these values, but C3 plant bulk $\delta^{13}C$ also showed the expected positive correlation (slope = 0.7‰/1000m, $r^2 = 0.3710$, $p = 0.0095$) between increase in elevation and ^{13}C enrichment. Isotopic data for plants collected on Mt. Gongga in China from Chen *et al.* (Figure 4) at altitudes below 2000m show evidence of the presence of C4 plant material due to their ^{13}C enrichment, but above that elevation (which should be populated primarily by C3 plants)[33, 49] there is good agreement

with the direction and magnitude of the altitude effect on C3 plant $\delta^{13}C$ seen in the Rio Beni. Note that Chen *et al.*'s average values exhibit much of the same variability observed for individual plant samples in the Rio Beni (i.e. fluctuations between 3000-4000m).

Lipid concentrations

The concentration patterns of fatty acids extracted from both C3 and C4 plants exhibited the expected[16, 25] even-over-odd carbon chain length preference (see Appendix for graphs). In plant samples the short-chain FAMEs C_{16} and C_{18} were typically the most abundant, a trend also observed in the sediment samples. However, while this is due to biosynthetic preference in plants, in sediments some of the enrichment in these short-chain FAMEs is likely due to in-river or in-soil production by microbial or algal activity.[12]

CPI and ACL values varied from plant to plant, with no clear trends within plant type categories. Plant CPI ranged from 3.12 to 23.48 with an average value of 12.75. Plant ACL ranged from 25.4 to 30.0, with an average of 27.6. These values are in the expected range; plant CPI is typically high (>5) showing the even-over-odd preference typical of leaf wax fatty acids,[26] while these compounds typically have an ACL in the range of 26-30.[23]

Lipid isotopes

The $\delta^{13}C$ values for plant samples showed a great deal of variability between chain lengths—on the order of 4-6‰—but there were no regular trends of enrichment or depletion by chain length (Appendix). Weighted averages of the

$\delta^{13}C$ signatures for even carbon number C_{24}-C_{30} FAs for each sample were used to allow comparison between plants, and of plants to sediments.

As expected,[17, 35, 49] the weighted averages for C4 plants were significantly enriched in ^{13}C relative to C3 plants (Figure 4). The overall average of lipid $\delta^{13}C$ was -20.61‰ for C4 plants and -33.37‰ for C3 plants, indicating fractionation of lipids relative to the average bulk values for C3 and C4 bulk tissue of approximately -4 to -8‰. These values are on the low end of the expected range of lipid offsets from biomass, which are typically in the -7 to -9‰ range.[48] With only 4 C4 samples to examine it was not possible to determine if there is a meaningful trend in their FA isotopic distribution with elevation. The 24 C3 samples show a positive trend (slope = 0.5‰/1000 m, $r^2 = 0.1202$, $p = 0.097$) in their FA $\delta^{13}C$ values, though it is obscured by a great deal of variability, as seen from the poor p-value. The FA trend is in the same direction as the bulk trend, though the FA trend is about 0.2‰ less pronounced than that seen for the bulk samples.

A literature search looking for potential sources of the high plant variability revealed that many ferns follow a CAM biosynthetic pathway rather than a C3 pathway.[50-52] CAM plants take up and metabolize CO_2 differently than C3 and C4 plants, leading to a wide range of variability in their $\delta^{13}C$ signatures[21, 53] With this information in hand it seemed reasonable to separate ferns from C3 plants for the purposes of this study. A trend line for C3 plants without the inclusion of data from fern samples yielded a slope of 0.6‰/1000m ($r^2 = 0.1985$,

p = 0.038), a trend which is closer to the magnitude of C3 elevation effects found in the literature, and one with much greater statistical significance.

Initial plant deuterium data (Figure 5) exhibit a great deal of variability with some evidence of the expected[20, 31, 32] trend of increasing deuterium depletion at higher altitudes (-8.2‰/1000 m, r^2=0.1533, p = 0.065). Previous studies have found that plants and plant FAs typically follow the δD depletion of their growth water as elevation increases (a trend on the order of -20‰/1000 m).[32, 34, 35] Plant wax-derived soil *n*-alkanes have been shown to be depleted by approximately -22.7‰/1000m.[54] The deuterium elevation-related fractionation effect observed for the initial plant samples is approximately half that seen in prior studies; analysis of more plants may help to reduce the variability and increase the strength of the trend.

The high variability observed for plant $\delta^{13}C$ and δD is due to interplant variability in metabolism and is typical of studies of this type.[17, 20, 35, 36, 49] It has been suggested that high interplant variability in δD at the same elevation may be due not only to differences in plant metabolism, but to microclimates which affect rates of envirotranspiration, and by extension, plant D/H fractionation.[55] The high interplant variability in $\delta^{13}C$ present at 820m spans almost the same range as the entire elevation effect (Figure 4). The magnitude of variability for both stable isotope measures could be problematic. However, interplant variability at a given altitude should yield a clearer trend upon analysis of more plant samples. The plant isotope signatures should also average out when materials enter and mix in

the river, so that sediments should more closely reflect the plant average for the elevation of origin. This type of averaging has been seen in previous studies of soil plant-derived *n*-alkanes in China[56] and soil plant-derived FAs in Japan.[17] While interplant variability precludes the ability to pinpoint the exact altitude of OC origin, plant-wax lipids should still be a useful proxy for tracing the general trend of OC movement.

II. Sediments

Prior research by Aalto *et al*.[38] suggests that the sediment core (Core 30 LFS 1500) contains sediment deposited by at least three separate flood events. The most recent flood event deposited the sediment found in the 52-56 cm and 56-58 cm horizons. The 187-189 cm and 191-193 cm horizons represent another, older flood, while the 239-241 cm and 243-245 cm horizons consist of sediment deposited by the oldest flood. Each of these sediments was size-fractionated to separate types of OC that were likely from different origins and subject to different transport and storage mechanisms.

Bulk properties

The percent organic carbon (%OC) was analyzed for the bulk sediment as well as for each fraction after separation (Figure 6-A). The values for the <63 μm fraction were extremely close to those for the bulk (pre-fractionation) sediment, which is unsurprising given that the <63μm fraction comprises 92.1-98.3 weight percent of the bulk fraction of each horizon (Table 2). Little variability in %OC

between depth horizons for the <63 μm fraction was apparent, with the values ranging from 1.03-0.39 %OC; the general trend appears to be towards lower %OC in the deeper horizons. The >63 μm fraction contained significantly higher concentrations of OC (~2-5%), with a wide range of variation. This is not surprising; it seems likely that the larger fraction may contain "chunks" of organic matter, perhaps even bits of leaf or other plant matter, as was found by Hedges *et al.* in larger particulate organic matter (CPOM).[41] The small fraction is likely more homogeneous because it contains smaller materials that are more easily mixed, like Hedges *et al.*'s FPOM.[41]

The same three fractions (bulk, <63 μm and >63 μm) were analyzed for their overall $\delta^{13}C$ signatures (Figure 6-B). The >63 μm fraction is more ^{13}C depleted ($\delta^{13}C$ -27.7 to -29.2‰) than both the bulk (-27.4 to -27.6‰) and <63 μm (-26.6 to -27.4‰) fractions. The >63 μm fraction had the greatest $\delta^{13}C$ variability – as it did for %OC, and likely for similar reasons – while the <63 μm fraction signatures by horizon closely resembled the patterns seen in the bulk sediments, but was overall slightly less depleted than the bulk fraction. This is logical given the substantially larger relative weight percent contribution of the <63 μm fraction to the bulk fraction (Table 2).

The $\delta^{13}C$ signatures of the <63 and >63 μm fractions exhibit a great deal of variability between the 187-189 cm and 191-193 cm horizons despite the fact that the bulk values for horizons deposited during the same flood event, as these were, typically have very similar properties. The heterogeneity of the OC in these

layers may indicate that the river's properties—namely the source(s) and processing of organic matter—changed during the flood event. Differences found in the size fractionated sediments fractions are invisible in the bulk sediment, and they support the findings of previous studies that 63 μm is a size cutoff that separates carbon pools with different chemical properties.[11, 39, 41]

Lipid concentrations

Both size fractions of the sediment samples in each depth horizon exhibited an even-over-odd preference for FAMEs with chain lengths $\geq C_{24}$ (Appendix, Figure A-2). This suggests that these sediment lipids are largely plant-derived, and are not highly degraded before their incorporation into sediments. The significantly lower concentrations seen in sediments compared to plants indicates that sediment OC is diluted by other, FA-poor sources of OC such as algal or microbial production.[12] Lipid concentrations in the <63 μm fraction are far lower than those seen in the >63 μm fraction, likely because the larger fraction is made up of recently and well-preserved plant litter, consistent with the findings of prior studies.[11]

No ACL differences between the two sediment size fractions were apparent, and the observed sediment ACL average of 27.4 was close to the average ACL for plant samples—another indication that the plant-derived lipids were well-preserved (Table 2).[23] CPI values for sediments varied between the large and small fractions. Overall average value for both fractions (9.21) was on the low end of the observed values for plants, and the average CPI for the large

fraction was closer (11.71) to the plant values than that of the small fraction (6.71). Even the lowest values are still quite high, and confirm that the OC is mostly plant derived; CPI values should be similar in source and sink if the lipids are not degraded, and the small fraction should consist of material that is more degraded than that found in the large fraction.[41]

Lipid isotopes

FA $\delta^{13}C$ values were on the whole more ^{13}C depleted than those of the bulk sediment (Figure 6). The small (<63 μm) fraction FAs are generally more ^{13}C enriched than the large (>63 μm) fraction FAs with the exception of the shallowest core horizon, which had more depleted ^{13}C values for the small fraction. The deeper (and correspondingly older) sediment FAs are generally more enriched in ^{13}C than those found closer to the surface with the notable exception of the 56-58 cm horizon <63μm fraction, which is the most enriched of the lipid samples. The overall average of the weighted averages for FA chain lengths from C_{24}-C_{30} of the <63 μm fraction for all horizons was -31.2‰, while for the >63 μm fraction the corresponding value was -33.7‰.

The depletion of the >63 μm fraction relative to the bulk and the <63 μm fractions suggests that the >63 μm fraction has a primarily lowland, primarily C3 origin. Several factors support the lowland origin hypothesis: the relatively undegraded plant material typically found in larger fractions is less likely to have traveled long distances.[12, 41] Further, this fraction's FA $\delta^{13}C$ values are very close to those of the C3 plants, which had an average over all elevations of -33.4‰. The

trend of ^{13}C enrichment at higher elevations should drive the average $\delta^{13}C$ values for plants that originate at greater altitudes away from those seen for this sediment size fraction. The overall enrichment of the <63 μm fraction, then, is likely due to the some combination of material from higher in the watershed and more input of C4-plant originated carbon. The C3/C4 effect is likely the cause of the extreme ^{13}C enrichment of the 56-58 cm <63 μm fraction, since the magnitude of the enrichment is approximately 2‰, or equal to an elevation effect of about 4000m based on the trend seen for the plant samples.

Similarly, the overall ^{13}C enrichment of the deeper sediments suggests that the FAs found in older sediments were either derived from plants which grew higher in the watershed or contained more input from C4 plants.[23, 29, 41, 49] If the enrichment is due to the elevation effect, it could indicate that earlier flood events carried material from higher in the watershed, and that the river dynamics have changed over the years: the river formerly carried large amounts of organic matter from high in the watershed and is now primarily depositing organic matter near its plant origin in the lowlands. This effect may not be due to long-term changes in river dynamics but to the character of an individual flood event in question. If the enrichment in older sediments is due to the presence of a great deal of C4 material, it could indicate that the plant community has shifted away from the C4 biosynthetic pathway and towards a C3 pathway. Rather than a true shift in plant community, it is possible that the organic matter which enters the river is due to erosion from lower portions of the watershed which contains more C4 plants. The

overall effect of enrichment with depth is likely due to some combination of changes in the elevation of origin of the organic matter and C4 enrichment; with data for only one sediment core it is not possible to be sure that the observed trend of enrichment with depth will be found in other cores. Separation of the C3/C4 plant mixing effect from the elevation signal should be made easier by the analysis of more plant samples, and the addition of more δD data from the sediment core.

Deuterium data for the bank sediment sample support the conclusion drawn from the $\delta^{13}C$ values: that the <63 μm fraction (which exhibits δD depletion relative to the >63 μm fraction) originates from more distant, higher elevation, and therefore more D-depleted, plant source. Deuterium analysis of all of the depth horizons for this sediment core and analysis of more sediment cores from different parts of the watershed will help to confirm these effects and put them into context.

III. Conclusions

As we hoped, leaf wax fatty acids from C3 plants exhibited evidence of both carbon and hydrogen isotopic fractionation trends with altitude. C4 plants were enriched in ^{13}C relative to C3 plants, which made it difficult to separate the effects of C3/C4 mixing from the elevation effect in sediment samples. Carbon and hydrogen isotopic signatures as well as ACL and CPI data support a plant wax origin for the long-chain fatty acids found in sediments. More deuterium data for sediment samples should help to separate the effects of the different factors

which contribute to their isotopic signatures.

Separation of sediments at 63 μm yields two fractions with distinct chemical properties. The $\delta^{13}C$ signatures of the >63 μm fraction suggest a local, low-altitude source of plant matter with significant amounts of C4 plant material. The $\delta^{13}C$ signatures of the <63 μm fraction, on the other hand, suggest a more distant source of largely C3 plant matter. The initial sediment δD data appear to support these conclusions.

There is an apparent trend towards increasing depletion with depth in the $\delta^{13}C$ data for the sediment core. This trend suggests that there may have been a change in the elevation from which most plant matter enters the river and/or plant biosynthetic pathway preference in the watershed over time. More δD data for this core and analysis of samples from other cores will help to confirm if this apparent trend is significant, and if it is, to determine the cause(s) underlying the change in isotopic signature.

Analysis of the plant samples and the initial sediment core indicate that the use of plant wax *n*-alkanoic acid isotope signatures as a biomarker proxy for the movement of OC is a potentially useful tool that merits further investigation. Combination of this biomarker study of the region with another isotopic study of the lignin-derived phenols extracted from the same sample suite should provide a more robust method for examining the carbon transport patterns of the region.

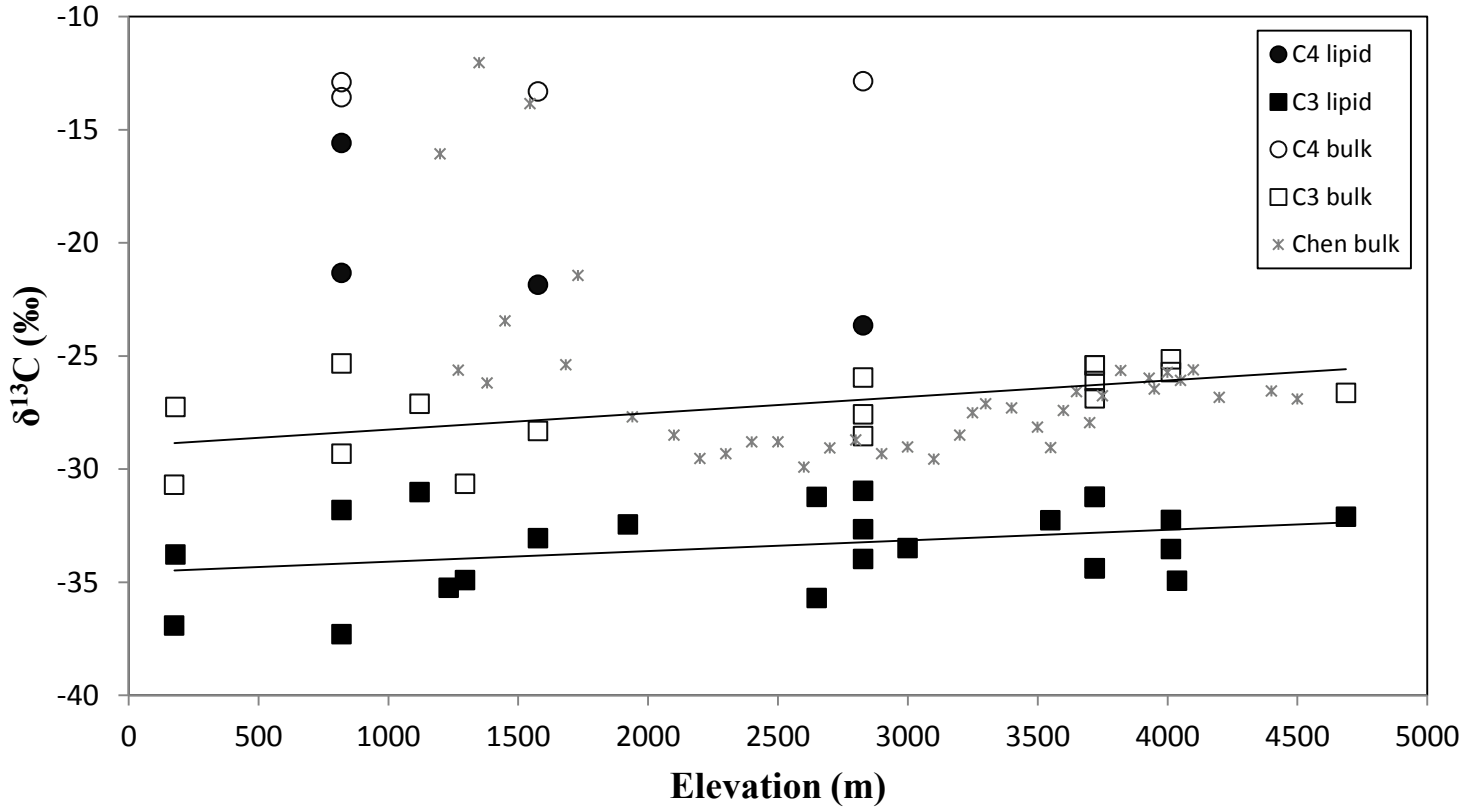

Figure 4: C3 and C4 plant $\delta^{13}C$ by elevation. The slope of the linear fit for the C3 plant FAs is 0.5‰/1000m (r^2 = 0.1202, p = 0.097) and the slope of the linear fit for the available C3 plant bulk (total organic carbon) data is 0.7‰/1000m (r^2 = 0.3710, p = 0.0095). The points from Chen et al.[33] represent the average values for plant total organic carbon $\delta^{13}C$ at each altitude on the eastern slope of Mt. Gongga, China.

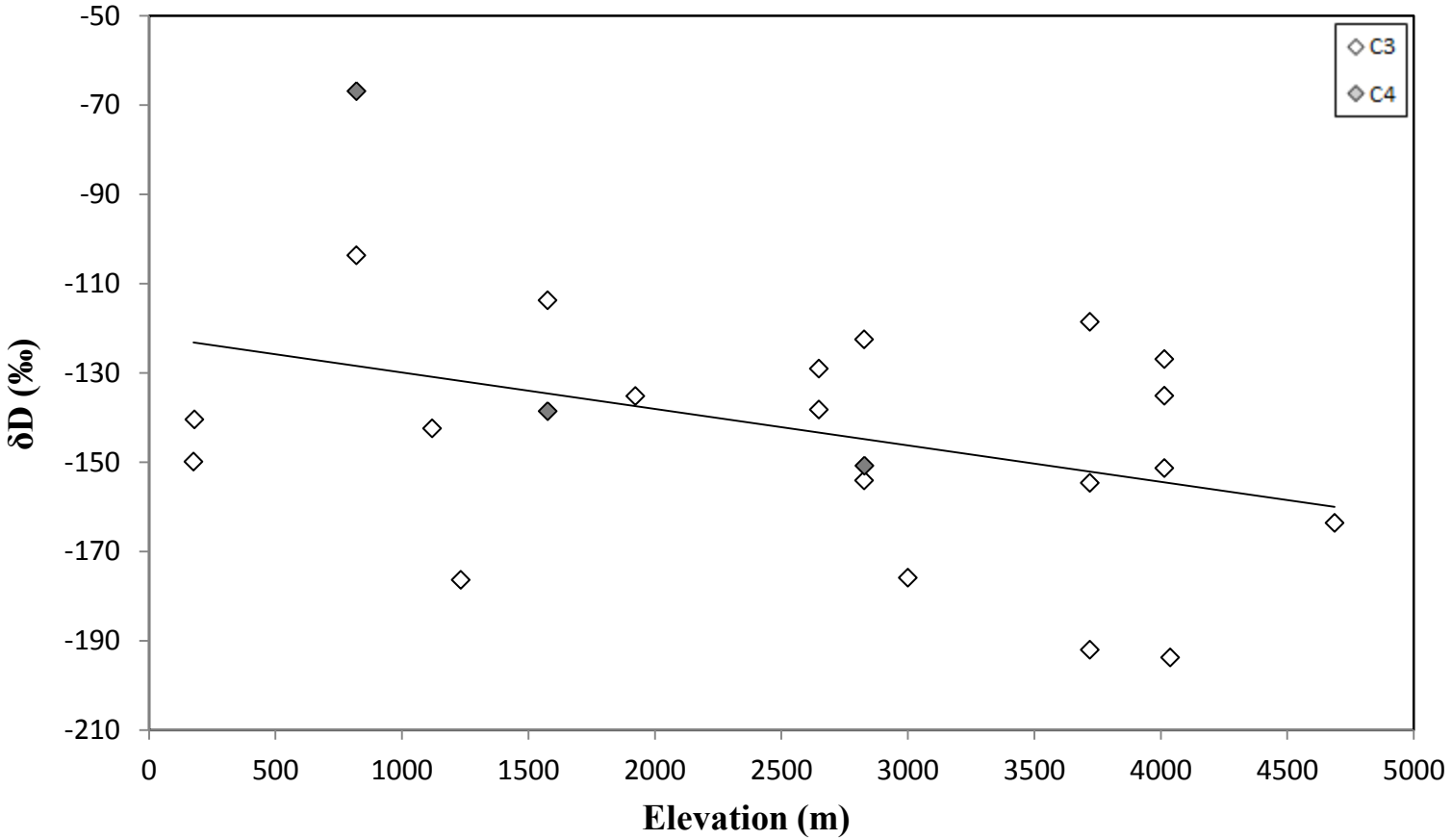

Figure 5: C3 & C4 plant fatty acid δD by elevation. Trend line for C3 plants has a slope of -8.2‰/1000m (r^2 = 0.1533, p = 0.065)

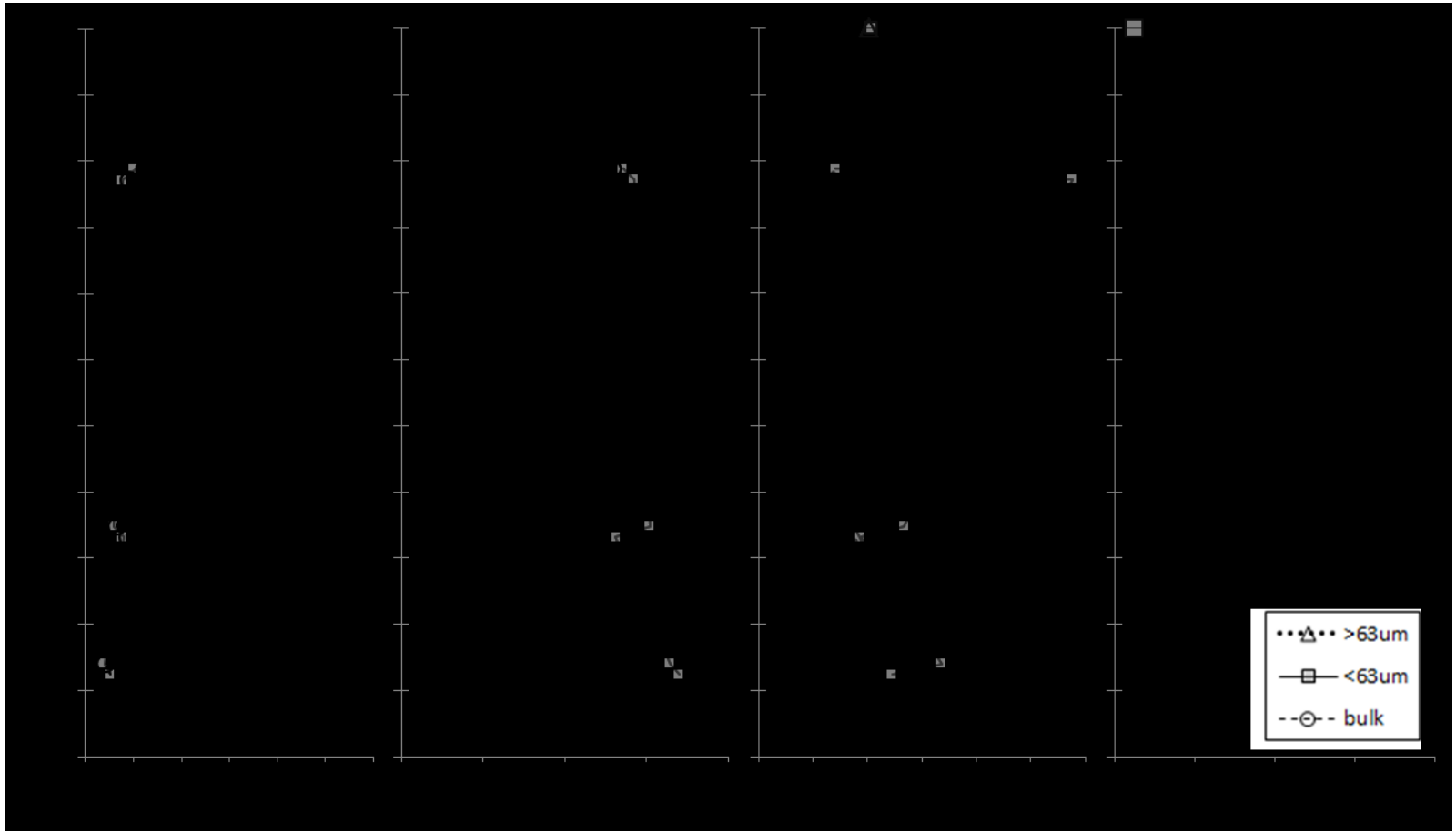

Figure 6: (a) weight percent OC, (b) $\delta^{13}C$ of total OC, (c) $\delta^{13}C$ of fatty acids, and (d) δD of fatty acids extracted from sediments at different depths in the sediment core (30 LFS 1500). Data shown at depth = 0 cm are from a bank deposit, not the sediment core.

Table 1: Plant sample description and organic geochemical data

Sample ID	Plant type	Elevation (m)	Latitude (°S)	Longitude (°W)	%OC*	Bulk $\delta^{13}C$ (‰)	FA $\delta^{13}C$ (‰)*	FA δD (‰)*	ACL*	CPI*
A26.2	tree/shrub	176	-13.84582	-67.46116	37.73	-30.70	-36.92	-149.91	27.32	9.40
RFC50_1000m.1	grass	180	-13.63984	-67.35459	42.26	-27.26	-33.78	-140.42	29.71	7.25
A33.10	C4 grass	820	-15.79614	-67.50719	39.92	-13.57	-21.34	-66.86	29.64	18.58
A33.11	tree/shrub	820	-15.79614	-67.50719	46.59	-25.34	-31.81	n.d.*	27.58	9.44
A33.12	tree/shrub	820	-15.79614	-67.50719	34.06	-29.33	-37.29	-103.68	28.43	16.01
A33.9	C4 grass	820	-15.79614	-67.50719	36.93	-12.91	-15.59	n.d.	26.49	8.11
A10.2	fern	1120	-15.51636	-67.95743	45.90	-27.11	-31.03	-142.47	27.24	23.48
A155.8	grass	1233	-15.29827	-68.44048	43.56	n.d.	-35.24	-176.40	29.48	19.80
A31.2	tree/shrub	1296	-15.66362	-67.46354	41.94	-30.65	-34.91	n.d.	27.42	12.29
A36.3	C4 grass	1576	-16.20935	-67.75500	39.70	-13.32	-21.86	-138.55	29.94	4.94
A36.5	tree/shrub	1576	-16.20935	-67.75500	39.18	-28.32	-33.06	-113.72	27.98	13.76
A168.7	tree/shrub	1923	-16.49925	-67.42606	n.d.	n.d.	-32.45	-135.22	26.66	14.45
A140.3	tree/shrub	2649	-15.76671	-68.64763	46.64	n.d.	-31.23	-138.21	26.50	14.34
A140.5	tree/shrub	2649	-15.76671	-68.64763	45.33	n.d.	-35.71	-129.05	26.23	3.10
A2.1	fern	2828	-16.29611	-67.81870	44.68	-27.59	-30.96	n.d.	26.03	20.78
A2.2	grass	2828	-16.29611	-67.81870	42.35	-25.95	-32.66	-154.12	29.26	10.69
A2.3	tree/shrub	2828	-16.29611	-67.81870	43.26	-28.55	-33.97	-122.52	26.81	20.92
A2.4	C4 grass	2828	-16.29611	-67.81870	37.19	-12.86	-23.65	-150.77	27.67	6.95
A137.2	grass	3000	-15.79364	-68.65274	39.52	n.d.	-33.49	-175.92	27.54	10.34
A137.5	herb	3000	-15.79364	-68.65274	42.50	n.d.	n.d.	n.d.	25.38	20.07
A136.7	tree/shrub	3549	-15.83008	-68.64181	49.05	n.d.	-32.26	n.d.	26.44	14.92
A1.1	grass	3720	-16.32740	-67.95526	37.19	-26.88	-34.38	-154.67	28.52	10.22
A1.2	grass	3720	-16.32740	-67.95526	40.44	-26.11	-34.39	-192.06	27.16	9.69
A1.3	tree/shrub	3720	-16.32740	-67.95526	45.81	-25.42	-31.24	-118.61	27.43	17.21
A40.5	tree/shrub	3720	-16.44965	-68.09042	46.27	-26.67	-31.24	-126.92	26.87	14.26
A40.3	grass	4014	-16.44965	-68.09042	24.66	-25.71	-33.53	-135.16	27.94	13.83

Sample ID	Plant type	Elevation (m)	Latitude (°S)	Longitude (°W)	%OC*	Bulk $\delta^{13}C$ (‰)	FA $\delta^{13}C$ (‰)*	FA δD (‰)*	ACL*	CPI*
A40.6	herb	4014	-16.44965	-68.09042	39.36	-25.15	-32.25	-151.34	26.84	12.20
A135.2	grass	4037	-15.86268	-68.63939	41.06	n.d.	-34.94	n.d.	26.67	10.36
A135.3	moss/carpet	4037	-15.86268	-68.63939	39.60	n.d.	n.d.	-193.79	27.61	8.82
A39.2	grass	4687	-16.33987	-68.03820	32.52	-26.64	-32.11	-163.63	26.66	9.65

** %OC represents the weight percent organic carbon in the bulk sample, FA $\delta^{13}C$ is the weighted average of $\delta^{13}C$ values for the C_{24}-C_{30} fatty acids, FA δD is the weighted average of δD values for the C_{24}-C_{30} fatty acids, ACL = average chain length; CPI = carbon preference index, n.d. = value not determined for this sample*

Table 2: Description of samples from sediment core 30 LFS 1500 and bank sediment deposit

Depth horizon (cm)	Size fraction	Weight %	% OC*	Bulk $\delta^{13}C$ (‰)	FA $\delta^{13}C$ (‰)*	ACL*	CPI*
Bank deposit	Bulk	-	0.86	-27.5	-	-	-
	<63 µm	87.1	0.67	-27.3	-32.85	26.49	3.28
	>63 µm	12.9	1.82	-27.8	-32.90	27.87	2.606
52-54	Bulk	-	1.26	-27.42	-	-	-
	<63 µm	96.7	1.03	-27.29	-34.19	27.37	10.85
	>63 µm	3.3	5.07	-28.56	-33.29	27.51	9.46
56-58	Bulk	-	0.94	-27.64	-	-	-
	<63 µm	96.3	0.78	-27.15	-25.48	26.73	7.00
	>63 µm	3.7	2.91	-28.75	-35.62	27.37	10.85
187-189	Bulk	-	0.67	-27.40	-	-	-
	<63 µm	96.2	0.60	-26.96	-31.67	29.03	11.40
	>63 µm	3.8	3.85	-29.21	-33.83	27.16	20.72
191-193	Bulk	-	0.91	-27.49	-	-	-
	<63 µm	92.1	0.79	-27.38	-33.25	27.64	4.04
	>63 µm	7.9	2.78	-28.03	-33.45	27.57	3.64
239-241	Bulk	-	0.43	-27.14	-	-	-
	<63 µm	98.2	0.39	-26.71	-30.27	27.37	5.35
	>63 µm	1.8	2.50	-28.25	-33.13	27.45	8.66
243-245	Bulk	-	0.53	-26.85	-	-	-
	<63 µm	98.3	0.52	-26.60	-32.10	26.99	10.44
	>63 µm	1.7	2.18	-27.70	-32.97	27.05	8.11

**%OC represents the weight percent organic carbon in the bulk sample, FA $\delta^{13}C$ is the weighted average of $\delta^{13}C$ values for the C_{24}-C_{30} fatty acids, ACL = average chain length; CPI = carbon preference index, n.d. = value not determined for this sample*

APPENDIX: CONCENTRATION AND $\delta^{13}C$ GRAPHS FOR PLANT AND SEDIMENT SAMPLES

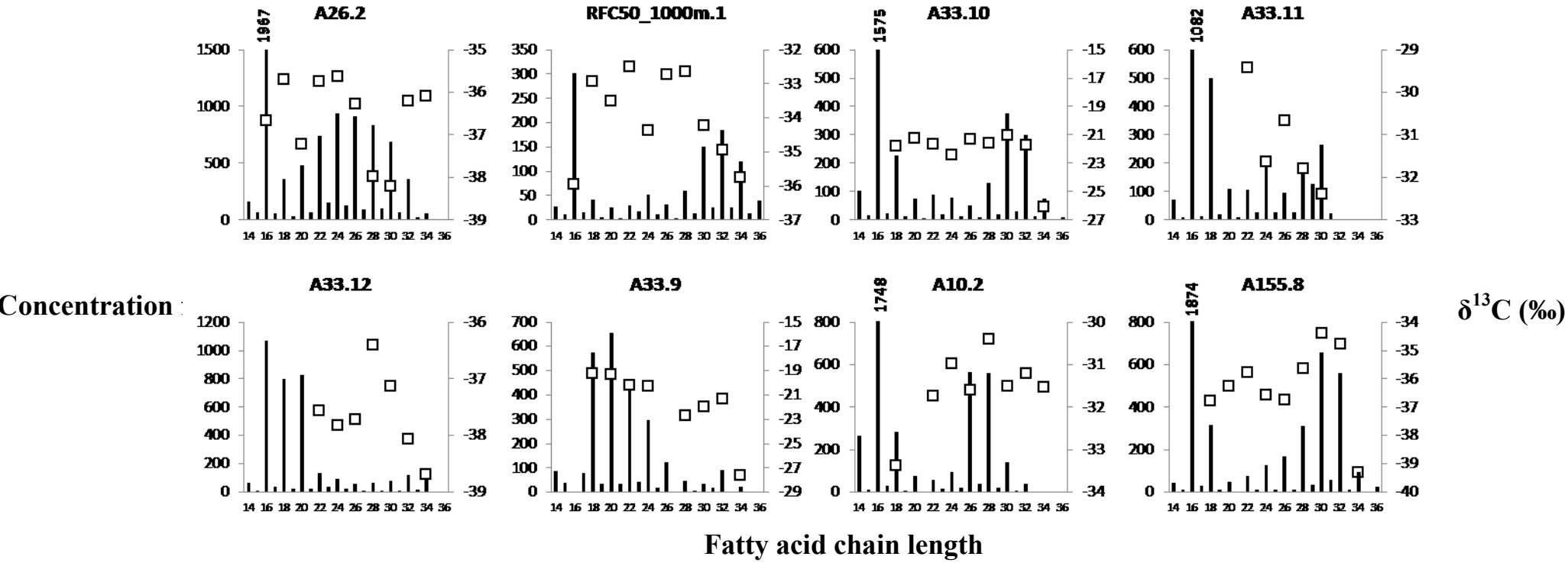

Figure A-1: Plant sample fatty acid concentration (bars) and $\delta^{13}C$ (squares) by chain length.

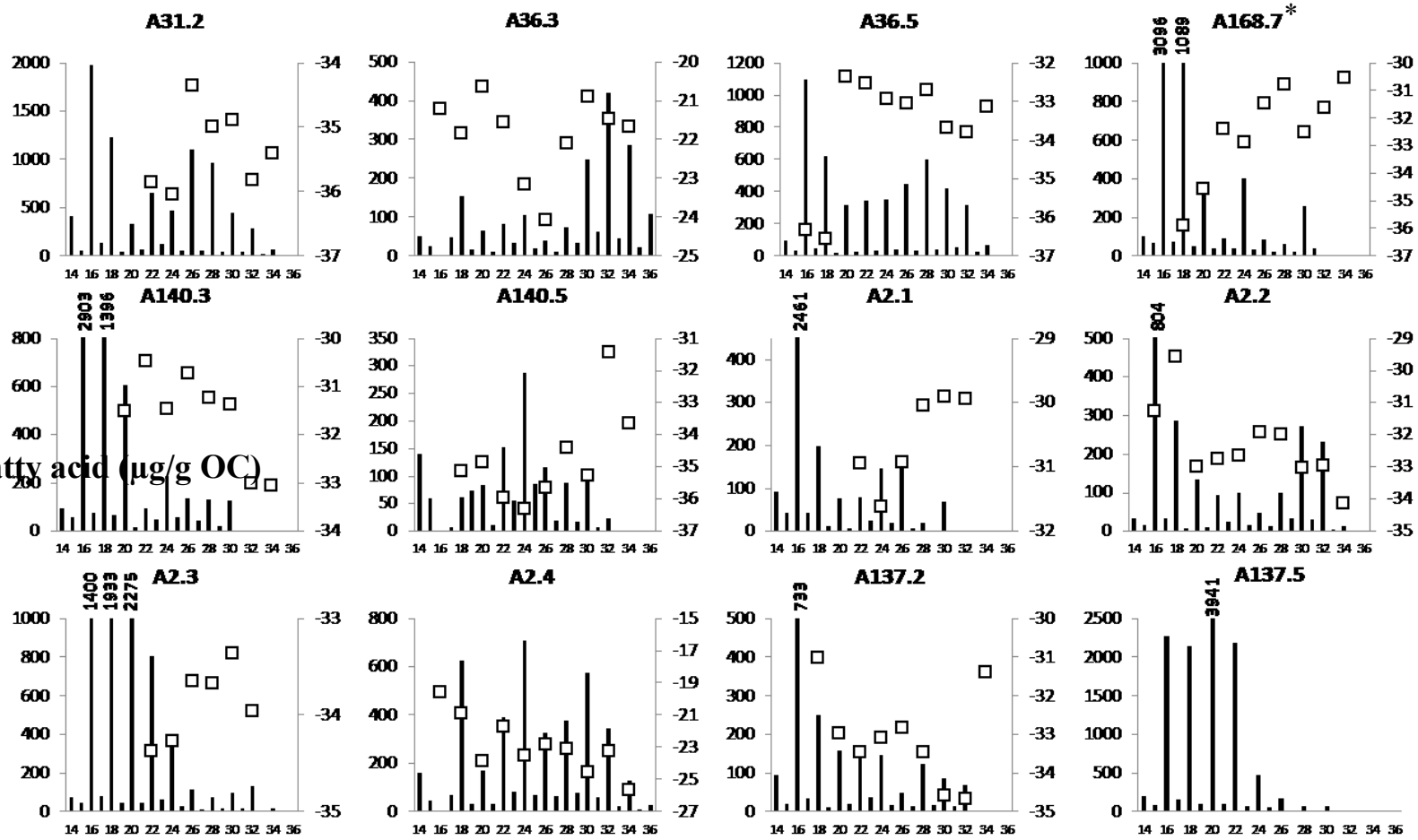

Figure A-1 continued

**Concentrations for A168.7are estimated; bulk %OC data were unavailable for this sample.*

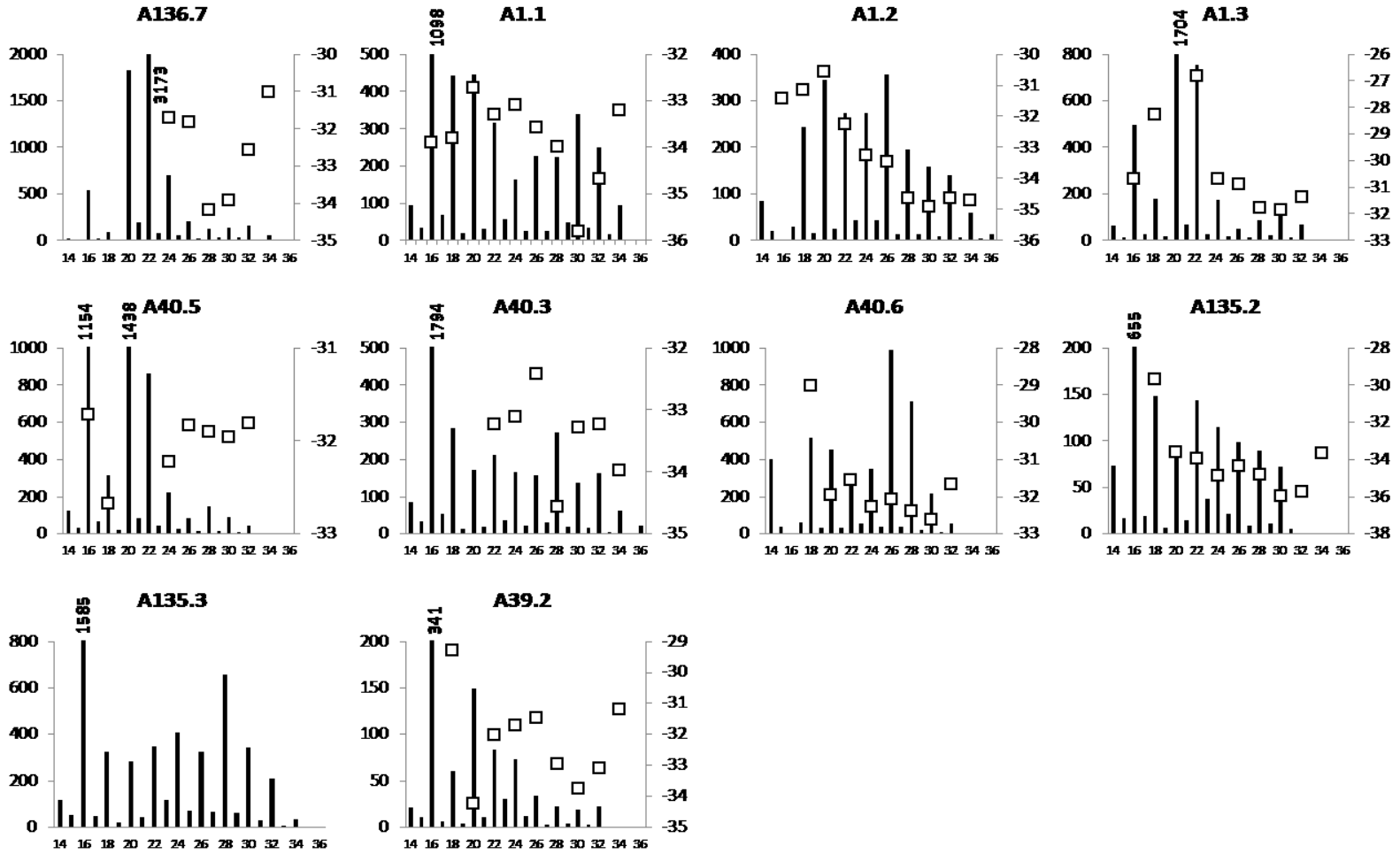

Figure A-1 continued

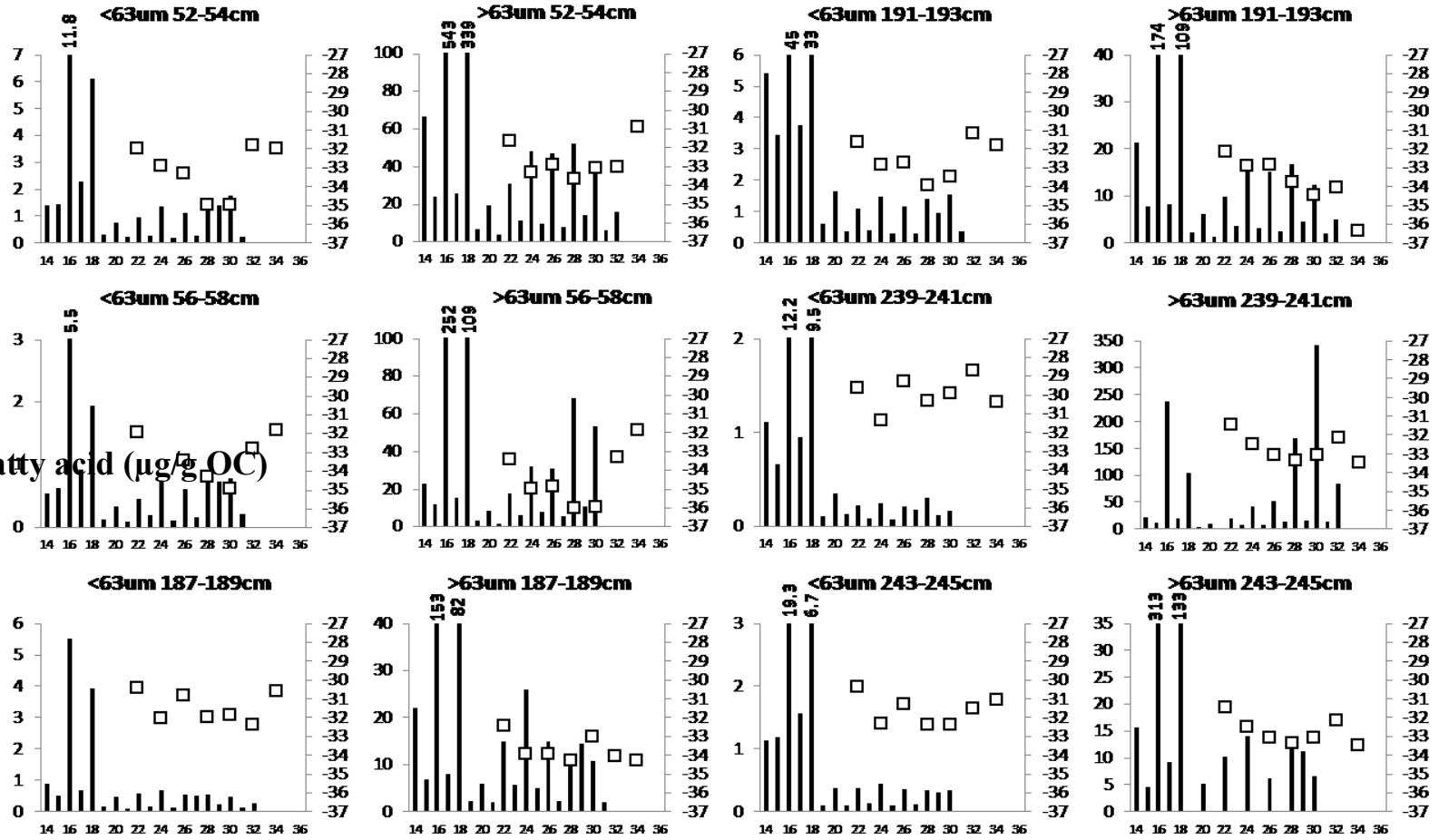

Concentration fatty acid (µg/g OC)

$\delta^{13}C$ (‰)

Fatty acid chain length

Figure A-2: Sediment core (30 LFS 1500) and bank sample sample fatty acid concentration (bars) and $\delta^{13}C$ (squares) by chain length

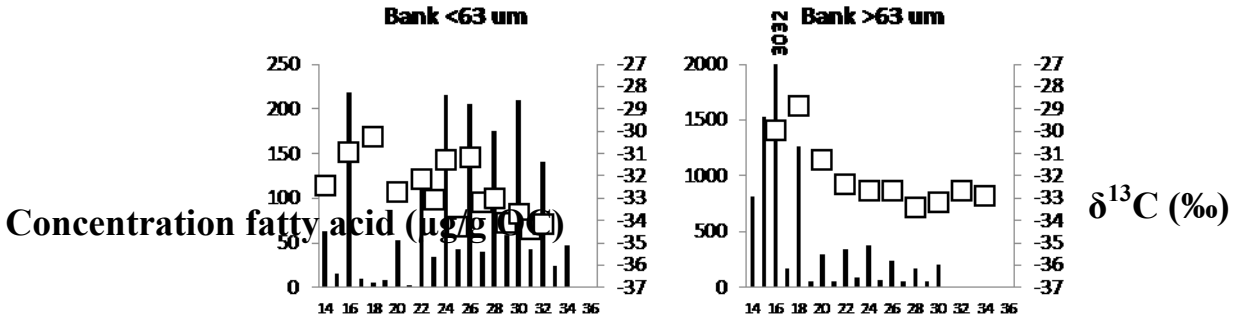

Figure A-2 continued

REFERENCES

(1) Janzen, H. H. Carbon cycling in earth systems—a soil science perspective. *Agriculture, Ecosystems and Environment* **2004***, 104*, 399-417.

(2) Cox, P. M.; Betts, R. A.; Jones, C. D.; Spall, S. A.; Totterdell, I. J. Acceleration of global warming due to carbon-cycle feedbacks in a coupled climate model. *Nature* **2000***, 408*, 184-187.

(3) Houghton, R. A. *The Contemporary Carbon Cycle;* Schesinger, W. H., Holland, H. D. and Turekian, K. K., Eds.; Treatise on Geochemistry: Biogeochemistry; Elsevier-Pergamon: Oxford, U.K., 2003; Vol. 8, pp 473-513.

(4) Schlesinger, W. H. *Biogeochemistry - An analysis of global change* Academic Press: San Diego, CA, 1997; 588 pp.

(5) Chapin, F. S., III; Matson, P. A.; Mooney, H. A. *Principles of Terrestrial Ecosystem Ecology* Springer: USA, 2002; 436 pp.

(6) Stallard, R. F. Terrestrial sedimentation and the carbon cycle: Coupling weathering and erosion to carbon burial. *Global Biogeochem. Cycles* **1998***, 12*, 231-257.

(7) Shaver, G. R.; Canadell, J.; Chapin III, F. S.; Gurevitch, J.; Harte, J.; Henry, G.; Ineson, P.; Jonasson, S.; Melillo, J.; Pitelka, L.; Rustad, L. Global Warming and Terrestrial Ecosystems: A Conceptual Framework for Analysis. *BioScience* **2000***, 50(10)*, 871-882.

(8) DeCelles, P. G.; Giles, K. A. Foreland basin systems. *Basin Research* **1996***, 8*, 105-123.

(9) Keil, R. G.; Montlucon, D. B.; Prahl, F. G.; Hedges, J. I. Sorptive Preservation of Labile Organic Matter in Marine Sediments. *Nature* **1994**, *370*, 549-552.

(10) Richey, J. E.; Melack, J. M.; Aufdenkampe, A. K.; Ballester, V. M.; Hess, L. L. Outgassing from Amazonian rivers and wetlands as a large tropical source of atmospheric CO_2. *Nature* **2002**, *416*, 617-620.

(11) Hedges, J. I.; Clark, W. A.; Quay, P. D.; Richey, J. E.; Devol, A. H.; de M. Santos, U. Compositions and fluxes of particulate organic material in the Amazon River. *Limnol. Oceanogr.* **1986**, *1*, 717-738.

(12) Hedges, J. I.; Keil, R. G.; Benner, R. What happens to terrestrial organic matter in the ocean? *Org. Geochem.* **1997**, *27(5/6)*, 195-212.

(13) Cole, J. J.; Caraco, N. F. Carbon in catchments: connecting terrestrial carbon losses with aquatic metabolism. *Mar. Freshwater Res.* **2001**, *52(1)*, 101-110.

(14) Houghton, R. A. Why are estimates of the terrestrial carbon balance so different? *Global Change Biol.* **2003**, *9*, 500-509.

(15) Eglinton, G.; Pancost, R. Immortal Molecules. *Geoscientist* **2004**, *14*, 4-16.

(16) Eglinton, T. I.; Eglinton, G. Molecular proxies for paleoclimatology. *Earth Planet. Sci. Lett.* **2008**, *275*, 1-16.

(17) Chikaraishi, Y.; Naraoka, H. Carbon and hydrogen isotope variation of plant biomarkers in a plant–soil system. *Chem. Geol.* **2006**, *231*, 190-202.

(18) Goni, M. A.; Yunker, M. B.; Macdonald, R. W.; Eglinton, T. I. Distribution and sources of organic biomarkers in arctic sediments from the Mackenzie River and Beaufort Shelf. *Mar. Chem.* **2000**, *71*, 23-51.

(19) Hedges, J. I.; et al. The molecularly-uncharacterized component of nonliving organic matter in natural environments. *Org. Geochem.* **2000**, *31*, 945-958.

(20) Sachse, D.; Radke, J.; Gleixner, G. δD values of individual *n*-alkanes from terrestrial plants along a climatic gradient - implications for the sedimentary biomarker record. *Org. Geochem.* **2006**, *37*, 469-483.

(21) Chikaraishi, Y.; Naraoka, H.; Poulson, S. R. Hydrogen and carbon isotopic fractionations of lipid biosynthesis among terrestrial (C3, C4 and CAM) and aquatic plants. *Phytochemistry* **2004**, *65*, 1369-1381.

(22) Quenea, K.; Derenne, S.; Largeau, C.; Rumpel, C.; Mariotti, A. Variation in lipid relative abundance and composition among different particle size fractions of a forest soil. *Org. Geochem.* **2004***, 35*, 1355-1370.

(23) Jansen, B.; Nierop, K. G. J.; Hageman, J. A.; Cleef, A. M.; Verstraten, J. M. The straight-chain lipid biomarker composition of plant species responsible for the dominant biomass production along two altitudinal transects in the Ecuadorian Andes. *Org. Geochem.* **2006***, 37*, 1514-1536.

(24) Jaffe, R.; Elismi, T.; Cabrera, A. C. Organic geochemistry of seasonally flooded rain forest soils: molecular composition and early diagenesis of lipid components. *Org. Geochem.* **1996***, 25*, 9-17.

(25) Eglinton, G.; Hamilton, R. J. Leaf Epicuticular Waxes. *Science* **1967***, 156*, 1322-1334.

(26) Jansen, B.; Nierop, K.G.J. Methyl ketones in high altitude Ecuadorian Andosols confirm excellent conservation of plant-specific *n*-alkane patterns. *Org. Geochem.* **2009***, 40*, 61-69.

(27) Hoefs, J. *Stable Isotope Geochemistry* Springer-Verlag: Berlin, 1997; 201 pp.

(28) Ehleringer, J. R.; Cerling, T. E. Stable Isotopes. *Encyclopedia of global environmental change* **2002***, 2*, 544-550.

(29) Körner, C.; Farquhar, G. D.; Wong, S. C. Carbon isotope discrimination by plants follows latitudinal and altitudinal trends. *Oecologica* **1991***, 88*, 30-40.

(30) Hou, J.; D'Andrea, W. J.; Huang, Y. S. Can sedimentary leaf waxes record D/H ratios of continental precipitation? Field, model, and experimental assessments. *Geochim. Cosmochim. Acta* **2008***, 72*, 3503-3517.

(31) Poage, M. A.; Chamberlain, C. P. Empirical relationships between elevation and the stable isotope composition of the precipitation and surface waters: considerations for studies of paleoelevation change. *Am. J. Sci.* **2001***, 301*, 1-15.

(32) Sessions, A. L.; Burgoyne, T. W.; Schimmelmann, A.; Hayesa, J. M. Fractionation of hydrogen isotopes in lipid biosynthesis. *Org. Geochem.* **1999**, 1193-1200.

(33) Chen, P. N.; Wang, G. A.; Han, J. M.; Liu, X. J.; Liu, M. $\delta^{13}C$ difference between plants and soil organic matter along the eastern slope of Mount Gongga. *Chinese Sci. Bull.* **2010***, 55*, 55-62.

(34) Smith, F. A.; Freeman, K. H. Influence of physiology and climate on δD of leaf wax *n*-alkanes from C3 and C4 grasses. *Geochim. Cosmochim. Acta* **2006***, 70*, 1172-1187.

(35) Chikaraishi, Y.; Naraoka, H. $\delta^{13}C$ and δD relationships among three *n*-alkyl compound classes (*n*-alkanoic acid, *n*-alkane and *n*-alkanol) of terrestrial higher plants. *Org. Geochem.* **2006***, 38*, 198-215.

(36) Wei, K.; Jia, G. Soil *n*-alkane $\delta^{13}C$ along a mountain slope as an integrator of altitude effect on plant species $\delta^{13}C$. *Geophys. Res. Lett.* **2009***, 36*, L11401-L11406.

(37) Gautier, E.; Brunstein, D.; Vauchel, P.; Roulet, M.; Fuertes, O.; Guyot, J. L.; Darozzes, J.; Bourrel, L. Temporal relations between meander deformation, water discharge and sediment fluxes in the floodplain of the Rio Beni (Bolivian Amazonia). *Earth Surf. Processes Landforms* **2006***, 32(2)*, 230-248.

(38) Aalto, R.; Maurice-Bourgoin, L.; Dunne, T.; Montgomery, D. R.; Nittrouer, C. A.; Guyot, J. L. Episodic sediment accumulation on Amazonian flood plains influenced by El Nino/Southern Oscillation. *Nature* **2003***, 425(6957)*, 493-487.

(39) Aufdenkampe, A.; Mayorga, E.; Hedges, J. I.; Llerena, C.; Quay, P. D.; Gudeman, J.; Krusche, A. V.; Richey, J. E. Organic matter in the Peruvian headwaters of the Amazon: Compositional evolution from the Andes to the lowland Amazon mainstem. *Org. Geochem.* **2007***, 38*, 337-364.

(40) Aufdenkampe, A. personal communication.

(41) Hedges, J. I.; Mayorga, E.; Tsamakis, E.; McClain, M. E.; Aufdenkampe, A.; Quay, P.; Richey, J. E.; Benner, R.; Opsahl, S.; Black, B.; Pimentel, T.; Quintanilla, J.; Maurice, L. Organic Matter in Bolivian Tributaries of the Amazon River: A Comparison to the Lower Mainstream. *Limnol. Oceanogr.* **2000***, 45(7)*, 1449-1466.

(42) Keil, R. G.; Mayer, L. E.; Quay, P. D.; Richey, J. E.; Hedges, J. I. Loss of organic matter from riverine particles in deltas. *Geochim. Cosmochim. Acta* **1997***, 61(7)*, 1507-1511.

(43) Guyot, J. L.; Jouanneau, J. M.; Quintanilla, J.; Wasson, J. G. Dissolved and suspended sediment loads exported from the Andes by the Beni River (Bolivian Amazonia), during a flood. *Geodinimica Acta* **1993***, 6*, 233-241.

(44) Coplen, T. B.; Brand, W. A.; Gehre, M.; Groning, M.; Meijer, H. A. J.; Toman, B.; Verkouteren, R. M. New guidelines for $\delta^{13}C$ measurements. *Anal. Chem.* **2006***, 78*, 2439-2441.

(45) Whiteside, J. H.; Olsen, P. E.; Eglinton, T.; Brookfield, M. E.; Sambrotto, R. N. Compound-specific carbon isotopes from Earth's largest flood basalt eruptions directly linked to the end-Triassic mass extinction. *Proc. Natl. Acad. Sci. U. S. A.* **2010***, 107 (15)*, 6721-6725.

(46) Goodman, K. J. Hardware Modifications to an Isotope Ratio Mass Spectrometer Continuous-Flow Interface Yielding Improved Signal, Resolution, and Maintenance. *Anal. Chem.* **1998***, 70*, 833-837.

(47) Johnson, C. personal communication.

(48) Drenzek, N. J.; Montluçon, D. B.; Yunker, M. B.; Macdonald, R. W.; Eglinton, T. I. Constraints on the origin of sedimentary organic carbon in the Beaufort Sea from coupled molecular ^{13}C and ^{14}C measurements. *Mar. Chem.* **2007***, 103*, 146-162.

(49) Li, J. Z.; Wang, G. A.; Liu, X. Z.; Han, J. M.; Liu, M.; Liu, X. J. Variations in carbon isotope ratios of C-3 plants and distribution of C-4 plants along an altitudinal transect on the eastern slope of Mount Gongga. *Science in China Series D: Earth Sciences* **2009***, 52*, 1714-1723.

(50) Wong, S. C.; Hew, C. S. Diffusive Resistance, Titratable Acidity, and CO2 Fixation in Two Tropical Epiphytic Ferns. *American Fern Society* **1976***, 66*, 121-124.

(51) Zotz, G. How prevalent is crassulacean acid metabolism among vascular epiphytes? *Oecologia* **2004***, 138*, 184-192.

(52) Ricalde, M. F.; Andrade, J. L.; Duran, R.; Dupuy, J. M.; Sima, J. L.; Us-Santamarıa, R.; Santiago, L. S. Environmental regulation of carbon isotope compositionand crassulacean acid metabolism in three plant communitiesalong a water availability gradient. *Oecologia* **2010***, 164*, 871-880.

(53) O'Leary, M. H. Carbon Isotopes in Photosynthesis. *Bioscience* **1988***, 38*, pp. 328-336.

(54) Luo, P.; Peng, P.; Gleixner, G.; Zheng, Z.; Pang, Z.; Ding, Z. Empirical relationship between leaf wax *n*-alkane δD and altitude in the Wuyi,

Shennongjia and Tianshan Mountains, China: Implications for paleoaltimetry. *Earth Planet. Sci. Lett.* **2011***, 301*, 285-296.

(55) Hou, J.; D'Andrea, W. J.; Macdonald, D.; Huang, Y. S. Hydrogen isotopic variability in leaf waxes among terrestrial and aquatic plants around Blood Pond, Massachusetts (USA). *Org. Geochem.* **2007***, 38*, 977-984.

(56) Jia, G.; Wei, K.; Chen, F.; Peng, P. Soil *n*-alkane δD vs. altitude gradients along Mount Gongga, China. *Geochim. Cosmochim. Acta* **2008***, 72*, 5165-5174.